



Published in final edited form as:

Nature. ; 478(7368): 241–245. doi:10.1038/nature10437.

Molecular Organization of Vomeronasal Chemoreception

Yoh Isogai^{1,2}, Sheng Si¹, Lorena Pont-Lezica^{1,3}, Taralyn Tan¹, Vikrant Kapoor¹, Venkatesh N. Murthy¹, and Catherine Dulac^{1,2}

¹Department of Molecular and Cellular Biology, Center for Brain Science, Harvard University

²Howard Hughes Medical Institute

Abstract

The vomeronasal organ (VNO) plays a key role in mediating the social and defensive responses of many terrestrial vertebrates to species- and sex-specific chemosignals¹. Over 250 putative pheromone receptors have been identified in the mouse VNO^{2,3}, but the nature of the signals detected by individual VNO receptors has not yet been elucidated. In order to gain insight into the molecular logic of VNO detection leading to mating, aggression, or defensive responses, we sought to uncover the response profiles of individual vomeronasal receptors to a wide range of animal cues. We describe here the repertoire of ethological and physiological stimuli detected by a large number of individual vomeronasal receptors, and define a global map of vomeronasal signal detection. We demonstrate that the two classes of vomeronasal receptors V1Rs and V2Rs use fundamentally different strategies to encode chemosensory information, and that distinct receptor subfamilies have evolved towards the specific recognition of certain animal groups or chemical structures. The association of large subsets of vomeronasal receptors with cognate, ethologically and physiologically relevant stimuli establishes the molecular foundation of vomeronasal information coding, and opens new avenues for further investigating the neural mechanisms underlying behavior specificity.

The discovery of large receptor families mediating olfactory and vomeronasal chemosensation has offered a unique opportunity to decode the molecular logic by which environmental information influences animal behavior^{3,4}. The vomeronasal organ (VNO) of rodents plays a critical role in identifying sex- and species- specific chemical cues and in mediating mating, territorial aggression, defensive responses to predators and associated endocrine changes^{1,5}. With rare exceptions^{6,7,8}, the molecular identity of VNO receptors (VRs) recognizing distinct animal cues is unknown, thus limiting the ability to explore the

Users may view, print, copy, download and text and data- mine the content in such documents, for the purposes of academic research, subject always to the full Conditions of use: http://www.nature.com/authors/editorial_policies/license.html#terms

Correspondence and requests for materials should be addressed to C.D. (dulac@fas.harvard.edu).

³Current address: Ecole Normale Supérieure; Paris, France.

Supplementary Information is linked to the online version of the paper at www.nature.com/nature.

Author contributions

Y.I. and C.D. designed the study. Y.I., S.S., and T.T. designed and generated RNA probes, performed RNA in situ hybridization, and analyzed data. L.P.-L. performed pilot experiments for figure 1 and produced recombinant ESP1. Y.I. and V.K. performed calcium imaging and electrophysiology. V.M. supervised physiology experiments. Y.I. and C.D. wrote the paper.

Author information

The authors declare no competing financial interests.

sensory mechanisms underlying behavioral specificity. Prior studies suggested that vomeronasal detection is extremely sensitive and narrowly tuned to male, female, or heterospecific cues^{5,9,10,11}, but they have not allowed the identification of the activated receptors. We describe here a robust and high-throughput molecular readout of vomeronasal activation that enabled us to uncover the receptor specificity of 88 individual VRs to a vast range of ethologically relevant cues. These results establish the molecular and functional framework underlying vomeronasal signaling.

In initial experiments, we exposed female mice to male or clean bedding and assessed the upregulation of the immediate early genes (IEGs) *Arc*, *c-Fos*, *c-Jun*, *Egr1*, *FosB*, and *Nr4a1* by in situ hybridization on VNO tissue. Our data show that the sensitivity of *Egr1* induction following semiochemical exposure far exceeds that of other IEGs (Fig. 1a, b) (60.1 ± 7.1 cells per 0.2 mm^2 for *Egr1*, 7.9 ± 1.9 cells per 0.2 mm^2 for *c-Fos*). Indeed *c-Fos*, an IEG used in previous VNO stimulation studies labels only a subset of *Egr1* positive cells (Supplementary fig. 1). In *TrpC2*^{-/-} mutants, in which VNO activation is genetically impaired¹², *Egr1* induction after semiochemical exposure is completely abolished (n=3), demonstrating the specificity of *Egr1* activation following sensory stimulation (Fig. 1c).

We then exposed animals to 29 distinct ethologically relevant cues^{5,13}. Male and female bedding from different mouse subspecies and wild-derived strains, as well as a variety of heterospecific cues from sympatric competitors and predators robustly induced *Egr1* expression in the VNO (Fig. 2a). Remarkably, food-related insect stimuli and cues from presumably neutral species such as woodchuck failed to generate VNO activation.

V1R and V2R neurons were equally activated by a large variety of stimuli as judged by co-labeling of *Egr1* with *Gai2*, a marker of V1R-expressing neurons^{14,15} (Fig. 2b, Supplementary fig. 2a). Interestingly, simultaneous exposure to multiple cues from the same class of animals (e.g., *Peromyscus* species, reptiles, or predatory birds) did not significantly increase the number of *Egr1*+ cells when compared to activation by a single stimulus ($p > 0.4$, two tailed t-test when the strongest of each stimulus class was compared to the corresponding mix), indicating that neuronal populations activated by related animals are largely overlapping (Fig. 2a). In contrast, simultaneous exposure to all heterospecific stimuli significantly increased *Egr1*+ cells from 5 to 10 % per cue to up to ~30 % ($p < 0.01$, two tailed t-test), indicating that distinct heterospecific cues have different response profiles. Moreover, while mouse bedding activated 5 to 7 % of VNO neurons in animals of the opposite sex, mixes of conspecific and heterospecific scents activated ~35 % of neurons (Fig. 2a) suggesting that receptors activated by both types of cues are also largely distinct.

To assess *Egr1* as readout of VNO activation, we compared it to cue-evoked neuronal responses visualized by the genetically encoded calcium indicator G-CaMP3¹⁶. Strikingly, *Egr1* and G-CaMP3 reported remarkably similar patterns of activities in the basal, or basal plus apical VNO neuroepithelium following exposure to rat and snake stimuli, respectively (Fig. 2c-e), confirming *Egr1* induction as an exquisitely sensitive and accurate marker of VNO neuronal activation.

Next, we developed a high-throughput platform to uncover the receptors activated by specific cues. With the exception of widely expressed V2R2 receptors¹⁷, vomeronasal neurons are thought to express a unique receptor gene from the V1Rs or V2Rs. We generated 209 RNA probes that specifically identify individual or subgroups of VRs by in situ hybridization. A collection of clade-specific probes was designed to target all receptor sequences within each of the 8 distinct V1R or V2R clades (Fig. 2f). Probes with higher specificity that readily distinguish a single or few closely related VR sequences were designed based on divergent 5'UTR/intron¹⁸ and 3'UTR regions in VR genes. The specificity of these probes for closely related VRs was validated by dual color in situ hybridization (Supplementary fig. 3). While detecting all VRs at single gene resolution was technically impossible, altogether our probes targeted 139 distinct VRs with specificity of a single or at most few genes.

We then used a hierarchical approach to systematically uncover VRs activated by distinct cues (Supplementary fig. 2b, 4). First, the co-expression of *Egr1* with either *Gai2*, *Gao* or formyl peptide receptors (FPRs)^{19,20} identified the nature of the activated neurons as expressing a V1R, V2R or FPR, respectively. Most stimuli activated both V1R- and V2R-expressing neurons, while few activated only V1R- (hawk and owls) or V2R-expressing cells (rat, fox and male mouse cues in females) (Supplementary table 1). We found no activation of FPR-expressing cells. We then assessed the specific V1R or V2R clades associated with the activated neurons (Fig. 2f, Supplementary fig. 2c). Interestingly, some clades appeared specifically stimulated by a distinct class of cues, for example V1Rd and V2R clades 4 and 7 by sex-specific cues. Subsequently, receptor specific probes were used to unmask the exact molecular identity of the *Egr1*+ cells. By collecting data from 9,948 VNO slices, each containing approximately 1000 neurons, we succeeded in the identification of 88 receptors (56 V1Rs and 32 V2Rs, 78 single and 10 unresolved receptors) associated with distinct cues (Supplementary fig. 5, Supplementary table 1, 2). Importantly, these receptors span most V1R and V2R clades, thus generating the most comprehensive functional map of vomeronasal receptors to date.

The vomeronasal system plays an essential role in regulating sex-specific behaviors. Previous reports suggest that vomeronasal neurons detect sex-specific cues in mouse urine, tear and saliva^{9,10,13,21,22}, and *Vmn2r116* (or *V2Rp5*) was identified as detecting the male pheromone *ESP1*⁶ (Supplementary fig. 6). Our strategy uncovered 28 receptors (25 single, 3 unresolved) detecting mouse cues, among which 26 detecting sex-specific cues (Fig. 3a–c, Supplementary table 1). Only two receptors (*V1ri9*, *V1ri10*) responded to both male and female mouse cues, consistent with the desensitization of IEG induction in vivo by self-secreted stimuli⁶. Four receptors (*V1re2*, *V1re3*, *V1re6*, *V1rg6*) were selectively activated by female cues in males and females, while a larger set of V1Rs and V2Rs responded to female cues only in males (Fig. 3a–c, Supplementary table 1). In addition, responses to male-specific signals involved *Vmn2r116*, *Vmn2r28*, *Vmn2r15*, *Vmn2r16*, and *Vmn2r17* in males and females, *Vmn2r66* and *Vmn2r82* in females, and *Vmn2r84/85/86/87* and *Vmn2r88* in males (Fig. 3a–c, Supplementary table 1). Interestingly, no V1R was found to specifically respond to male cues. Thus, consistent with a previous report⁹, the detection of sex-specific cues appears to rely on a small and specific subset of VNO neurons, the identity

of which is now clearly established. This molecular logic is likely to underlie the initiation of sex-dependent behavioral interactions, such as male-male aggression and mating behaviors.

Vomeroneasal detection of heterospecific cues, or kairomones, is involved in the adaptive defensive behaviors^{5,13,23}. Indeed, rat bedding induces robust avoidance to the predator cues in TrpC2^{+/-} but not in TrpC2^{-/-} animals (Fig. 4g,h). Moreover TrpC2^{-/-} animals exhibited abnormal ingestive behavior of the predator bedding suggesting that VNO inputs also inhibits foraging^{24,25} (Supplementary fig. 7).

We report here the identity of 71 (63 single, 8 unresolved) receptors activated by heterospecific scents. Consistent with the distinct behavioral outputs generated by pheromones and kairomones, we found that only 11 receptors were common to both types of cues, while 60 were uniquely activated by heterospecific stimuli, and 17 by mouse cues only (Fig. 3d). The detection of kairomones thus emerges as a major function of the VNO^{5,13}. The identity of one of the identified receptor population for the detection of predator cues was confirmed independently by *Egr1* activation in cells expressing YFP under the V1Rh7 promoter²⁶ (Supplementary fig. 8). Further, loose patch recording of V1Rh7-YFP expressing neurons demonstrated significant increase in firing rates following exposure to ferret, but not to rat stimuli (1.732±0.170 Hz for ferret, 0.420±0.061 Hz for rat, n = 4) (Fig. 4d–f, Supplementary fig. 9).

Remarkably, some receptors show unique association with distinct classes of predators. Vmn2r89 and Vmn2r121 were exclusively activated by scents from snakes, V1rc10/11/12 by owls. Also, up to 70 % of V2R clade 5 neurons were activated by every mammalian predator tested, but not by sympatric non-predators (Fig. 4a–c, Supplementary fig. 5, 10). Moreover, each predator cue generated a distinct receptor signature: for example, rat stimuli activate Vmn2r59, Vmn2r60, Vmn2r61, Vmn2r108, and Vmn2r110, all within clade 8, while ferret cues activate V1rf5 and Vmn2r77/78/79, suggesting that the mouse VNO has the sensory machinery to discriminate predator species.

We then searched for receptors detecting sympatric species *Mus spicilegus* and *Mus musculus*, which diverged evolutionarily ~1.5 million years ago and do not breed in the wild^{27,28}. Receptors activated by *M. spicilegus* and *M. musculus* male cues appear mostly distinct, though often closely related (Supplementary fig. 5, 11). For example, Vmn2r8/9 and Vmn2r11, activated by *M. spicilegus*, and Vmn2r15, Vmn2r16 and Vmn2r17, activated by *M. musculus*, belong to clade 6 (Supplementary fig. 11b). Likewise, Vmn2r69 activated by *M. spicilegus* and Vmn2r66 by *M. musculus* belong to clade 3. Thus, through the activation of specialized receptors, *M. musculus* may readily discriminate scents emitted by closely related but reproductively incompatible species, a property that could be linked to the reproductive isolation of these species.

V1Rs and V2Rs are associated with segregated neural pathways²⁹, raising the possibility that fundamental functional differences may exist between the two families. Remarkably, our data suggest that V1Rs and V2Rs display different receptor properties. Nearly half of the V1Rs (27 out of 56) exhibit generalized activation by multiple cues (Fig. 3e), including

signals with apparent conflicting behavioral significance. For example, receptors within the V1Rh, V1Rc and V1Re clades were activated by mouse, predator and non-predator cues (Supplementary table 1, 2, Supplementary fig. 12). In contrast, most V2Rs (29 out of 32) are activated by cues reflecting a unique ethological context such as a male, female, or a given type of predator or non-predator. In addition, hierarchical clustering across all identified receptors revealed clear segregation between V1Rs and V2Rs (Supplementary fig. 5). These results suggest that V1R and V2R pathways may encode different types of information: individual V2Rs appear uniquely poised to encode information about the identity of emitters with clear behavioral significance, for example the sex of a conspecific or the predator or competitor nature of a heterospecific. In contrast, individual V1Rs may encode other forms of biologically relevant information.

To gain further insight into the molecular logic of V1R-mediated signaling, we investigated the detection of sulfated steroids, thought to account for 80 % of VNO neuronal activation by female urine³⁰ likely through V1Rs¹¹. Our data show that, when male mice were exposed to a mix of synthetic steroid sulfates, receptors from V1Ref and V1Rjk clades were specifically activated (Fig. 5a, b). We then tested individual compounds to attempt the pairing of specific steroid ligands with their cognate receptors. Corticosterone-21 sulfate (Q1570), a compound in female urine³⁰, strongly activated *V1re2* and more weakly *V1re6* cells (Fig. 5a, b). Both receptors were shown in earlier experiments to be specifically activated by female cues (Fig. 3a). In addition, we uncovered strong activation of V1rf3 by 17 β -estradiol sulfate (E1050) and V1rj2 by both E1050 and 5-androstene-3 β , 17 β -diol disulfate (A7864) (Fig. 5a), although these two receptors were not activated by female bedding, indicating that these steroids are not secreted under normal conditions.

Thus, our approach efficiently achieved single compound resolution, offering the unique opportunity to test the receptor specificity to a variety of individual chemicals. We further tested 4 sulfated estrogen compounds structurally related to E1050, and 3 additional sulfated pregnenes structurally related to Q1570. V1rf3 appeared broadly selective to estradiols, estriols, and related stereoisomers, regardless of sulfate positions, but did not respond to androgens or glucocorticoids (Fig. 5c). Interestingly, no other V1rf receptor was activated by these ligands. In contrast, V1rj2 was activated by androgens and estradiols but not estriols. Similarly, V1re2 and V1re6 selectively detected corticosteroids (Fig. 5d). Therefore, V1R receptors can distinguish distinct structural classes of steroids. Androgens, estrogens, and glucocorticoids are ubiquitous though sensitive reporters of the animal endocrine state. Our results thus suggest that V1Rs may serve as detectors of the physiological status of an animal.

In conclusion, our data have begun to uncover the molecular logic by which vomeronasal receptors of different families, clades, and receptor sequences extract biological information and trigger appropriate behavioral responses to animals of a given sex, species and physiological status. The collection of receptors uncovered in this study provides a molecular foundation to further dissect the neural circuits governing social and sexual communication in rodents.

Methods Summary

Stimulus exposure was conducted by introducing a subject animal (male or female CD-1, 8 to 14 weeks old) in a fresh cage containing distinct animal cues for 30 (for Fig. 1) or 40 min (for Fig. 2–5). The dissected VNOs were embedded in OCT (Tissue-Tek) and frozen in dry ice. Cryosections (16 μm) of VNO were subjected to RNA in situ hybridization using immediate early gene and VR probes.

Methods

Sampling of animal stimuli

Bedding materials used in this study are all freshly sampled from cages that house live animals (Harvard University, Harvard Museum of Natural History, Harvard Concord Field Station, Tufts University, Museum of Science, Boston, and New England Wildlife Center). Soiled bedding represents the most complete stimulus source of animals, which are also of ecological relevance. Bedding materials typically absorb a wide range of chemical stimuli excreted by animals, such as urine, feces, saliva, fur, and other gland secretions. Since different animals are housed in different environments, we flexibly adjusted the sampling procedures. For instance, chemosignals emitted by heterospecific mammals and birds (male rat, female fox, male ferret, female bobcat, male *Peromyscus*, male *Mus spicilegus*, male and female gerbils, male and female hamsters, male and female rabbits, woodchuck, pigeon, red tailed hawk, screech owl, and great horned owl) were sampled as soiled bedding (paper, woodchips or corn cob). For reptiles, we sampled feces, urate and other gland secretions absorbed in woodchips or paper. These bedding materials were directly used for exposure experiments (as described separately below). For aquatic animals such as alligators, only fecal pellets were sampled. For insect larvae, live animals were directly used for exposure experiments. Some predators such as snake and predatory birds were fed mice as part of their diet, and we took a great caution to avoid potential odor contamination. For example, upon bedding sampling we avoided areas where mouse carcass was present in animal cages. Second, to sample milk snake odor, which we extensively used for our study, we changed bedding after the feeding to avoid potential odor contamination from mice. We also tested materials from multiple individuals whenever possible. Judging from the number of *Egr1* positive cells, we did not find extensive individual variability in these samples. If multiple individuals are not available, especially for bobcat, hawk, and great horned owl, we tested stimulus samples from different collection dates. We stored these bedding materials at 4 °C for short term (one week) and –20 °C for long term. These materials, even when the amount of volatiles are significantly reduced, did not appreciably lose activities in robustly stimulating VSNs over long term storage at –20 °C.

For conspecific stimuli, to represent a potential diversity of chemical cues emitted by different subspecies of mice, we have collected bedding samples from 5 different strains of mice: BALB/c (Jackson Labs), PWD/PhJ (Jackson Labs), CAST/EiJ (Jackson Labs), Idaho³¹, and Chuuk³¹, and exposed as a mixture. It is known that mice secrete different vomeronasal cues reflecting physiological states of animals, for example, different phases of estrous⁸, prompting us to sample materials freshly from cages that house multiple animals over 1 week. Thus, conspecific stimuli used in our study likely contain chemosignals

secreted over different phases of the estrous cycles. We stored these materials at 4 °C for short term and -20 °C for long term.

Stimulus exposure

For most exposure experiments involving bedding stimuli, approximately 50 ml (in volume) of bedding containing animal cues were placed in a clean cage. We introduced a subject mouse (male or female CD-1, from 8 weeks to 14 weeks old, Charles River), which voluntarily made extensive direct contacts with introduced stimuli in freely behaving conditions. The animals were exposed to stimuli for 30 (for Fig. 1) or 40 min (for Fig. 2–5). Subsequently, the dissected VNOs were embedded in OCT (Tissue-Tek) and frozen in dry ice. VNO cryosections (16 µm) were used for RNA in situ hybridization using immediate early gene and vomeronasal receptor probes. Control experiments were conducted using fresh bedding in an identical manner. For insect larvae exposure, 3~4 insect larvae were directly introduced to the cages. For alligator stimuli, a few fecal pellets were used. For heterospecific mix exposure experiments, ~100 ml mixture of following bedding sample was used: *Peromyscus* (*P. maniculatus*, *P. leucopus*, *P. polionotus*), mammalian predators (bobcat, fox, ferret, rat), avian predators (screech owl, great horned owl, red tail hawk), reptiles (rat snake, milk snake, rattlesnake, boa, alligator), and *Mus spicilegus*. For pure chemicals such as ESP1 and sulfated steroids, ~5 µl of Ringer's (in mM, 115 NaCl, 5 KCl, 2 CaCl₂, 2 MgCl₂, 25 NaHCO₃ and 5 HEPES) containing the stimuli were directly spotted on each nostril. Recombinant ESP1 was purified as a GST fusion protein overexpressed in *E. coli* using pET41 vector (Novagen), followed by thrombin cleavage to release the ESP1 peptide. 2 µg of the peptide was exposed to each animal.

Sulfated steroid exposure

Steroids were purchased from Steraloids. A mix of steroids (A6940, epitestosterone sodium sulfate; A7864, 5-androsten-3β, 17β-diol disulfate; E1050, 17β-estradiol sulfate; E0893, 17α-estradiol sulfate; P3817, allopregnanolone sulfate; P8200, epipregnanolone sulfate, Q1570, corticosterone 21-sulfate; Q3470, deoxycorticosterone 21-glucoside; each at 250 mM in Ringer's) were used for initial screens. Subsequently, individual steroids (Q1570; E1050; A7864; E0893; E0588, 17β-dihydroequilin 3-sodium sulfate; E1100, 17β-estradiol 3-sulfate; E2734, Estriol 17-sulfate; Q3910, hydrocortisone 21-sodium sulfate; Q2525, Cortisone 21-sulfate; Q5545, 3β-hydroxy-5-pregnen-20-one 3-sulfate) were used at 500 mM in Ringer's. 5 µl of steroid solution were spotted on each nostril of male CD-1 animals (8~14 weeks), and the animals were exposed to steroids for 40 min. Experiments were conducted for at least three animals.

Preparation of RNA probes

For immediate early gene probes, we have cloned cDNA of *Arc*, *c-Fos*, *c-Jun*, *Egr1*, *FosB*, *Nr4a1* in approximately 900 bp segments to pCRII-TOPO or pCR4-TOPO vector (Invitrogen). Antisense cRNA probes were synthesized using T3, T7, or Sp6 polymerases (Promega) and digoxigenin (DIG) or fluorescein (FITC) labeling mix (Roche) from PCR templates. All immediate early gene probes consisted of a cocktail of 2~3 probes to cover nearly the full length of these mRNAs.

For V1R clade specific probes, we have cloned full length coding sequence of V1R receptors (V1rab: a1, a2, a3, a4, a5, a6, a7, a8, b1, b2, b7, b8, b9; V1rc: c3, c8, c10, c16, c28; V1rd: d6, d9, d11, d12, d14, d22, Vmn1r167; V1ref: e1, e2, e3, e4, e6, e7, e8, e9, e10, e11, e12, e13, Vmn1r224, f1, f2, f3, f4, f5; V1rh: h1, h20; V1ri: i1, i3, i4, i5, i6, i8; V1rjk: j2, j3, k1) and combined these probes to generate a clade specific probe set. For V1rg receptors, ~1 kb 5' UTR/intron sequences of following genes were used: V1rg1, g2, g3, g4, g5, g6, g7, g8, g9, g10, g11, g12, Vmn1r77, which were combined with V1rl cDNA probe to generate the V1Rgl clade probe set.

To generate clade specific V2R probes, we have cloned first ~900 bp of annotated V2R receptor coding sequence (V2R clade 1: Vmn2r55; V2R clade 2: Vmn2r19, Vmn2r20, Vmn2r24; V2R clade 3: Vmn2r65, Vmn2r69, Vmn2r76, Vmn2r77; V2R clade 4: Vmn2r115; V2R clade 5: Vmn2r28, Vmn2r48; V2R clade 6: Vmn2r8, Vmn2r15, Vmn2r17, Vmn2r84, Vmn2r89, Vmn2r118; V2R clade 7: Vmn2r18, Vmn2r81, Vmn2r83, Vmn2r120; V2R clade 8: Vmn2r57 3'UTR probe, Vmn2r58, Vmn2r63, Vmn2r58, Vmn2r90, Vmn2r93, Vmn2r96, Vmn2r97, Vmn2r99, Vmn2r102, Vmn2r104, Vmn2r105, Vmn2r106, Vmn2r108, Vmn2r110, and Vmn2r64 3'UTR probe) and combined these probes to generate clade specific probe sets. To generate cRNA probes specific to individual V1R genes, we cloned ~1kb 5'UTR intron sequence of V1R genes to pCRII vector (Invitrogen). To produce cRNA probes specific to individual V2R receptors, we cloned ~600 bp of V2R 3'UTR segments. These RNA probes were first used to test mRNA expression. We found that some annotated vomeronasal receptor genes did not appear to be expressed since these RNA probes gave no discernible signals. For vomeronasal receptor genes which we could confirm the expression, we tested the specificity of these probes by dual color in situ hybridization using DIG and FITC probes and used for receptor mapping experiments. Probes generated in our study to detect specific receptors are listed in Supplementary table 1. The VR nomenclature was based on that of Genbank and Mouse Genome Informatics.

RNA in situ hybridization

Single color RNA in situ hybridization was conducted essentially as described³². We used DIG labeled cRNA probes at 2 ng/ml and used hybridization temperature of 65 °C for experiments conducted in Figure 1. For *Egr1* in situ hybridization experiments in Figure 2, we used 68 °C as hybridization temperature. Dual color fluorescence in situ hybridization was conducted in the following steps. First, the tissue was fixed in 4 % formaldehyde/1x PBS for 10 min, and washed with 3 times with 1x PBS for 3 min each. The tissues were treated with acetylation solution (0.1 M triethanolamine with 2.5 µl/ml acetic anhydride) for 10 min. After 3 washes with 1x PBS, each for 5 min, the slide was incubated with the pre-hybridization solution (50 % formamide, 5x SSC, 5x Denhardt's, 2.5 mg/ml yeast RNA, 0.5 mg/ml Herring sperm DNA) for 2 hrs. The hybridization buffer (4 % dextran sulfate, Millipore, added to pre-hybridization buffer) containing FITC labeled *Egr1* probes (a cocktail of three probes each at 50 pg/µl) and DIG labeled VR probes (at 0.5 ng/µl for cDNA probes, and 1 ng/µl for 5'UTR-intron and 3'UTR probes) was heated at 95 °C for 3 min and immediately chilled on ice for 5 min. The hybridization solution was applied to the slides, which were covered with parafilm and incubated in a sealed chamber for 16 hrs at 68 °C. Following hybridization, the slides were washed with 5x SSC once for 5 min, 0.2x SSC

three times, each for 20 min at 68 °C. Slides were washed at room temperature with 0.2x SSC for 5 min and subsequently with TNT buffer (100 mM Tris, pH 7.5, 150 mM NaCl, 0.05 % Tween 20) for 5 min.

After the post-hybridization washes, 200 µl of anti-FITC-POD (Roche, at 1/250 dilution in TNB blocking buffer, Perkin-Elmer) was applied and incubated for 3 hrs at room temperature. Slides were washed with TNT buffer for a total of 1 hr, with buffer exchanges every 10 min. The signal was developed using TSA biotin plus kit (Perkin Elmer), per manufacturer's protocol. The slides were washed with TNT buffer 3 times, each for 5 min, and subsequently treated with 3 % H₂O₂/1xPBS to kill residual peroxidase activity. Slides were washed again 3 times with 1x PBS and TNT, each for 5 min. DIG antibody solution (anti-DIG-POD, Roche, at 1/500 dilution, and Streptavidin-Alexa488, Invitrogen, at 1/250 dilution in TNB buffer) were applied to the slides and incubated overnight at 4 °C. After washing slides with TNT (6 times, 10 min each), the signal was developed using TSA Cy3 plus kit (Perkin Elmer) per manufacturer's protocol. Slides were washed with TNT (3 times, 5 min each and once for 1 hr), and tissues were mounted with Vectashield (Vector labs) containing 8 µg/ml DAPI. All the microscopy images were acquired using LSM510 or AxioImager Z2 (Zeiss).

Analysis of in situ hybridization images

For single color in situ hybridization images, quantitation was conducted using a minimum of 10 VNO sections per animal and 3 animals (Figure 1) or 3~4 animals (Figure 2). Since we found 0.2 mm² represent areas occupied by medial cryostat sections of the VNO and contain approximately 1000 VNO cells, we used the average number of *Egr1* positive cells per 0.2 mm² in Figure 1, and we converted these numbers to percentage of activated neurons among total VNO neurons in Figure 2. For dual color in situ hybridization, we quantitated the co-localization of *Egr1* and receptor signals over four sections per VNO, for a minimum of three animals. We then calculated the percentage of activated neurons in specific receptor neurons, for each odor class, and generated a co-localization matrix. In many cases, we found that individual receptor mapping is unnecessary when the hierarchical screen can unequivocally demonstrate that there are no activated neurons in specific receptor clades. In these cases, we input zero values to the co-localization matrix. For hierarchical clustering of the co-localization matrix, we used Cluster program (<http://bonsai.hgc.jp/~mdehoon/software/cluster/software.htm>), with average linkage in Euclidian distance. To generate the clustering diagram in Supplementary figure 4, we calculated the average number of receptor neurons per receptor in 12 sections and used this as a weight. The heat map and clustering dendrogram were generated using Java Treeview program (<http://jtreeview.sourceforge.net/>).

Behavioral assay

Male TrpC2 mice (+/- or -/-, 8~14 weeks old, ref. 12) were single-housed three days prior to the experiment in a manner blind to the experimenter. The behavior experiment was conducted by introducing 50 ml volume of fresh or rat bedding to one side of the cage, away from the nest area. The behaviors of the subject mice were video recorded and total contact time as well as ingestive behavior were scored by an individual blind to the genotype. We

defined ingestive behavior as animals engaged in ingestion while holding a food pellet with two forepaws.

Generation of OMP-GCaMP3 transgenic line

pJOMP plasmid containing the rat olfactory marker protein (OMP) genomic sequence³³ was modified so that the G-CaMP3 ORF sequence completely replaces the OMP ORF. Linearized vector was served for pronuclear injection (performed by Harvard Genome Modification Facility), and transgenic founders were further backcrossed to C57/Bl6 mice to establish an OMP-GCaMP3 line. This line expresses the transgene uniformly throughout the vomeronasal epithelium and showed no sign of reported cell toxicity¹⁵.

Calcium imaging on VNO slices

Calcium imaging was carried out essentially as described⁸, using 5~8 week old female OMP-GCaMP3 mice. The VNOs were acutely dissected, separated from bones, and embedded in 4 % low melting point agar in mACSF (in mM, 130 NaCl, 5 KCl, 1 MgCl₂, 2.5 CaCl₂, 1.25 NaH₂PO₄, 25 NaHCO₃, 10 Glucose). The coronal vibratome sections (200 μm) were cut, and slices were kept in continuously oxygenated mACSF for up to 8 hrs at room temperature. The flow rate of the stimulus was approximately 0.3 ml/min, and we delivered stimulus for 40 sec. All imaging was conducted at room temperature. The fluorescence changes due to calcium transients were monitored using a LSM710 microscope with a GaAsP detector (Zeiss). We used 1:100 of freshly sampled rat urine from 2~6 months old CD male Rats (Charles River) in mACSF. For snake stimuli, shredded snake bedding (*i.e.*, paper) was extracted with mACSF, filtered and used for stimulation. To quantify the number of activated cells, we first generated F images by subtracting an average of 20 sec frames corresponding to initial resting period from the raw images. We then created an average F image consisting of 10 sec frames corresponding to the maximum fluorescence interval (shown in the Fig. 2c). This operation significantly reduced the fluorescence signals from spontaneous activity, which is typically short (lasting 1~2 secs) and consists of small bursts, and enriched evoked activity, which is more sustained (more than 10 sec), larger rise in fluorescent intensity. The fluorescence traces of individual positive cells were further examined to confirm the sustained nature of the response. The number of activated cells was quantified using ImageJ. To quantify the number of viable cells during the imaging experiments, we counted the number of G-CaMP3 positive cells responsive to 40 mM KCl in mACSF.

Electrophysiology

Loose patch recordings: Loose patch recordings were performed at room temperature with a Multiclamp 700B (Axon Instruments). Data were recorded at 10 kHz, low pass filtered at 2 kHz and digitized with Digidata 1440A digitizer (Axon Instruments). Borosilicate glass (Sutter Instruments Co., O.D. 1.5 mm, I.D. 0.86 mm) patch pipettes (3-8 MΩ) were pulled on a Flaming/Brown micropipette puller (Sutter Instrument Co.). Same mACSF was used as the pipette solution. Data were acquired with pClamp and analyzed in Matlab. Pneumatic electronic valves (Clippard Instruments) were used to control the flow of stimuli. Electronic valves were controlled via digital output from the Digidata 1440 A digitizer. The valves

were opened for 20 seconds in every stimulated trial. For rat stimulus, we used 1:200 dilution of rat urine (male CD rats, Charles river, 2~6 month old) in mACSF. For ferret stimuli, ~50 ml volume of ferret bedding containing urine, feces, fur and gland excretions was extracted with 50 ml of mACSF overnight at 4 °C, then filtered and used for experiments.

Supplementary Material

Refer to Web version on PubMed Central for supplementary material.

Acknowledgements

The authors wish to acknowledge Heidi Fisher, Hopi Hoekstra, Emily Kay, Megan Kirchgessner, Naoshige Uchida, Alice Wang, Xiang-Dong Wang, Bunny Watson, Wenfei Tong, Harvard Museum of Natural History, Harvard Concord Field Station, Museum of Science, Boston, and New England Wildlife Center, for providing stimulus materials used in this study, Loren Looger for G-CaMP3 construct, Martin Wienisch, Foivos Markopoulos, Duncan Mak for help with electrophysiology and imaging experiments, Bernhard Goetze and the Harvard Center for Biological Imaging for help with microscopy. We also wish to thank members of the Dulac laboratory for critical reading of the manuscript, Svetlana Andreeva for technical support, and Renate Hellmiss for help with figure artwork. This work was supported by the NIDCD at the National Institute of Health, the Howard Hughes Medical Institute, and the Damon Runyon Cancer Research Foundation (Y.L., DRG-1981-08).

References

1. Dulac C, Torello AT. Molecular detection of pheromone signals in mammals: from genes to behaviour. *Nature Reviews Neuroscience*. 2003; 4:551–562. [PubMed: 12838330]
2. Zhang X, Marcucci F, Firestein S. High-throughput microarray detection of vomeronasal receptor gene expression in rodents. *Frontiers in Neuroscience*. 2010; 4:164. [PubMed: 21267422]
3. Dulac C, Axel R. A novel family of genes encoding putative pheromone receptors in mammals. *Cell*. 1995; 83:195–206. [PubMed: 7585937]
4. Buck L, Axel R. A novel multigene family may encode odorant receptors: a molecular basis for odor recognition. *Cell*. 1991; 65:175–187. [PubMed: 1840504]
5. Papes F, Logan DW, Stowers L. The vomeronasal organ mediates interspecies defensive behaviors through detection of protein pheromone homologs. *Cell*. 2010; 141:692–703. [PubMed: 20478258]
6. Haga S, et al. The male mouse pheromone ESP1 enhances female sexual receptive behaviour through a specific vomeronasal receptor. *Nature*. 2010; 466:118–122. [PubMed: 20596023]
7. Leinders-Zufall T, Ishii T, Mombaerts P, Zufall F, Boehm T. Structural requirements for the activation of vomeronasal sensory neurons by MHC peptides. *Nature Neuroscience*. 2009; 12:1551–1558. [PubMed: 19935653]
8. Boschat C, et al. Pheromone detection mediated by a V1r vomeronasal receptor. *Nature Neuroscience*. 2002; 5:1261–1262. [PubMed: 12436115]
9. He J, Ma L, Kim S, Nakai J, Yu CR. Encoding gender and individual information in the mouse vomeronasal organ. *Science*. 2008; 320:535–538. [PubMed: 18436787]
10. Leinders-Zufall T, et al. Ultrasensitive pheromone detection by mammalian vomeronasal neurons. *Nature*. 2000; 405:792–796. [PubMed: 10866200]
11. Holekamp TF, Turaga D, Holy TE. Fast three-dimensional fluorescence imaging of activity in neural populations by objective-coupled planar illumination microscopy. *Neuron*. 2008; 57:661–672. [PubMed: 18341987]
12. Stowers L, Holy TE, Meister M, Dulac C, Koentges G. Loss of sex discrimination and male-male aggression in mice deficient for TRP2. *Science*. 2002; 295:1493–1500. [PubMed: 11823606]
13. Ben-Shaul Y, Katz LC, Mooney R, Dulac C. In vivo vomeronasal stimulation reveals sensory encoding of conspecific and allospecific cues by the mouse accessory olfactory bulb. *Proceedings of the National Academy of Sciences of the United States of America*. 2010; 107:5172–5177. [PubMed: 20194746]

14. Berghard A, Buck LB. Sensory transduction in vomeronasal neurons: evidence for $G\alpha_o$, $G\alpha_{i2}$, and adenylyl cyclase II as major components of a pheromone signaling cascade. *Journal of Neuroscience*. 1996; 16:909–918. [PubMed: 8558259]
15. Jia C, Halpern M. Subclasses of vomeronasal receptor neurons: differential expression of G proteins ($G\alpha_{i2}$ and $G\alpha_o$) and segregated projections to the accessory olfactory bulb. *Brain research*. 1996; 719:117–128. [PubMed: 8782871]
16. Tian L, et al. Imaging neural activity in worms, flies and mice with improved GCaMP calcium indicators. *Nature Methods*. 2009; 6:875–881. [PubMed: 19898485]
17. Martini S, Silvotti L, Shirazi A, Ryba NJ, Tirindelli R. Co-expression of putative pheromone receptors in the sensory neurons of the vomeronasal organ. *Journal of Neuroscience*. 2001; 21:843–848. [PubMed: 11157070]
18. Stewart R, Lane RP. VIR promoters are well conserved and exhibit common putative regulatory motifs. *BMC Genomics*. 2007; 8:253. [PubMed: 17651493]
19. Liberles SD, et al. Formyl peptide receptors are candidate chemosensory receptors in the vomeronasal organ. *Proceedings of the National Academy of Sciences of the United States of America*. 2009; 106:9842–9847. [PubMed: 19497865]
20. Rivière S, Challet L, Fluegge D, Spehr M, Rodriguez I. Formyl peptide receptor-like proteins are a novel family of vomeronasal chemosensors. *Nature*. 2009; 459:574–577. [PubMed: 19387439]
21. Holy TE, Dulac C, Meister M. Responses of vomeronasal neurons to natural stimuli. *Science*. 2000; 289:1569–1572. [PubMed: 10968796]
22. Taha M, McMillon R, Napier A, Wekesa KS. Extracts from salivary glands stimulate aggression and inositol-1, 4, 5-triphosphate (IP₃) production in the vomeronasal organ of mice. *Physiology & Behavior*. 2009; 98:147–155. [PubMed: 19460393]
23. Samuelsen CL, Meredith M. The vomeronasal organ is required for the male mouse medial amygdala response to chemical-communication signals, as assessed by immediate early gene expression. *Neuroscience*. 2009; 164:1468–1476. [PubMed: 19778594]
24. Brown J, Kotler B, Smith R, Wirtz W. The effects of owl predation on the foraging behavior of heteromyid rodents. *Oecologia*. 1988; 76:408–415.
25. Sundell J, et al. Variation in predation risk and vole feeding behaviour: a field test of the risk allocation hypothesis. *Oecologia*. 2004; 139:157–162. [PubMed: 14730443]
26. Wagner S, Gresser AL, Torello AT, Dulac C. A multireceptor genetic approach uncovers an ordered integration of VNO sensory inputs in the accessory olfactory bulb. *Neuron*. 2006; 50:697–709. [PubMed: 16731509]
27. Chevret P, Veyrunes F, Britton-Davidian J. Molecular phylogeny of the genus *Mus* (Rodentia: Murinae) based on mitochondrial and nuclear data. *Biological Journal of the Linnean Society*. 2005; 84:417–427.
28. Guénet JL, Bonhomme F. Wild mice: an ever-increasing contribution to a popular mammalian model. *Trends Genet*. 2003; 19:24–31. [PubMed: 12493245]
29. Dulac C, Wagner S. Genetic analysis of brain circuits underlying pheromone signaling. *Annu Rev Genet*. 2006; 40:449–467. [PubMed: 16953793]
30. Nodari F, et al. Sulfated steroids as natural ligands of mouse pheromone-sensing neurons. *Journal of Neuroscience*. 2008; 28:6407–6418. [PubMed: 18562612]
31. Miller RA, et al. Mouse (*Mus musculus*) stocks derived from tropical islands: new models for genetic analysis of life-history traits. *Journal of Zoology*. 2000; 250:95–104.
32. Schaeren-Wiemers N, Gerfin-Moser A. A single protocol to detect transcripts of various types and expression levels in neural tissue and cultured cells: in situ hybridization using digoxigenin-labelled cRNA probes. *Histochemistry*. 1993; 100:431–440. [PubMed: 7512949]
33. Danciger E, Mettling C, Vidal M, Morris R, Margolis F. Olfactory marker protein gene: its structure and olfactory neuron-specific expression in transgenic mice. *Proceedings of the National Academy of Sciences of the United States of America*. 1989; 86:8565–8569. [PubMed: 2701951]

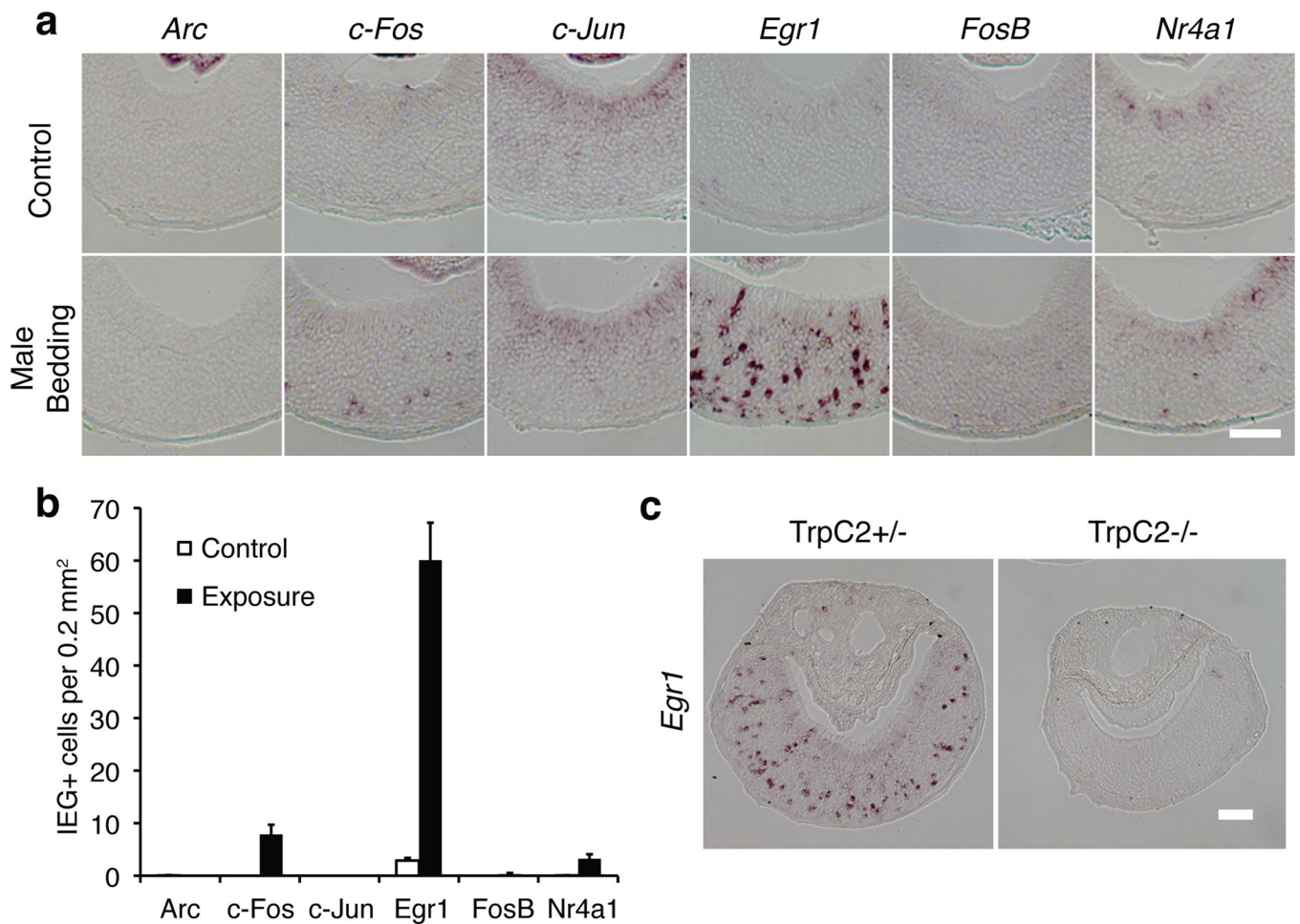


Figure 1. *Egr1* expression is robustly induced by pheromone-evoked VNO neuronal activation
 Female CD-1 mice were exposed to clean or male mouse bedding and their VNOs analyzed for expression of various immediate early genes (IEGs). **a**, In situ hybridization with RNA probes to *Arc*, *c-Fos*, *c-Jun*, *Egr1*, *FosB*, and *Nr4a1*. **b**, Numbers of IEG positive cells after bedding exposure (10 sections per VNO, n=3 animals). Error bars show s.e.m. **c**, *TrpC2*, a cation channel involved in VNO signal transduction is required for *Egr1* induction. Female *TrpC2*^{+/-} or *TrpC2*^{-/-} mice were exposed to male conspecific bedding and *Egr1* expression was visualized in the VNO. Bar, 100 μ m.

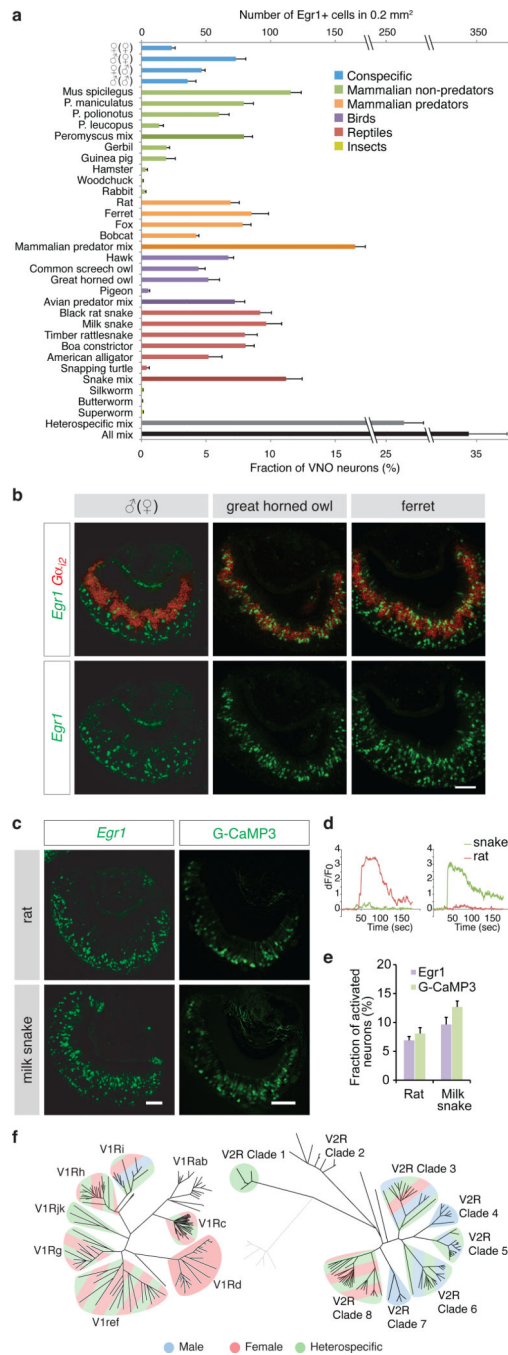


Figure 2. Widespread activation of VNO receptors by conspecific and heterospecific cues
a, Survey of ethologically relevant vomeronasal stimuli. Vomeronasal neural activation upon exposure to conspecific and heterospecific cues was visualized by *Egr1* induction and quantified. Detection of female cues by males is designated as ♀(♂). Unless specified, female mice were used. Mixed heterospecific cues activated *Egr1* in significantly more cells than individual stimuli ($p < 0.01$, two-tailed t-test). Co-exposure to heterospecific and conspecific stimuli (all mix, $n = 6$) resulted in significantly more *Egr1* positive cells ($p < 0.05$, two-tailed t-test). **b**, Widespread activation of VNO neurons by conspecific and

heterospecific cues. Shown are in situ hybridization with probes against *Gα_{i2}* (red) and *Egr1* (green). **c**, Comparison between *Egr1* and G-CaMP3-evoked signal in response to rat or milk snake chemosignals. G-CaMP3 images are 10 sec averages of F frames within stimulus period. **d**, Differential response profiles of neurons to rat or snake signals. Stimuli were perfused from 20 sec to 60 sec. **e**, Quantitative comparison between *Egr1* and G-CaMP3 evoked-signals. The percentage of activated cells identified by G-CaMP3 (n = 356 cells for rat stimuli, n = 566 cells for snake stimuli, 9 VNO slices from 3 animals) among those responsive to 40 mM KCl was plotted in the graph. Data for *Egr1* was taken from the Fig. 2a. The difference between *Egr1* and G-CaMP3 was not statistically significant (p>0.1, two tailed t-test). **f**, Clade-level maps of V1R (left) and V2R (right) activation show distinct clade specificity for male, female or heterospecific cues. Hatched patterns indicate response to multiple types of cues. Error bars are in s.e.m. Scale bars show 100 μm.

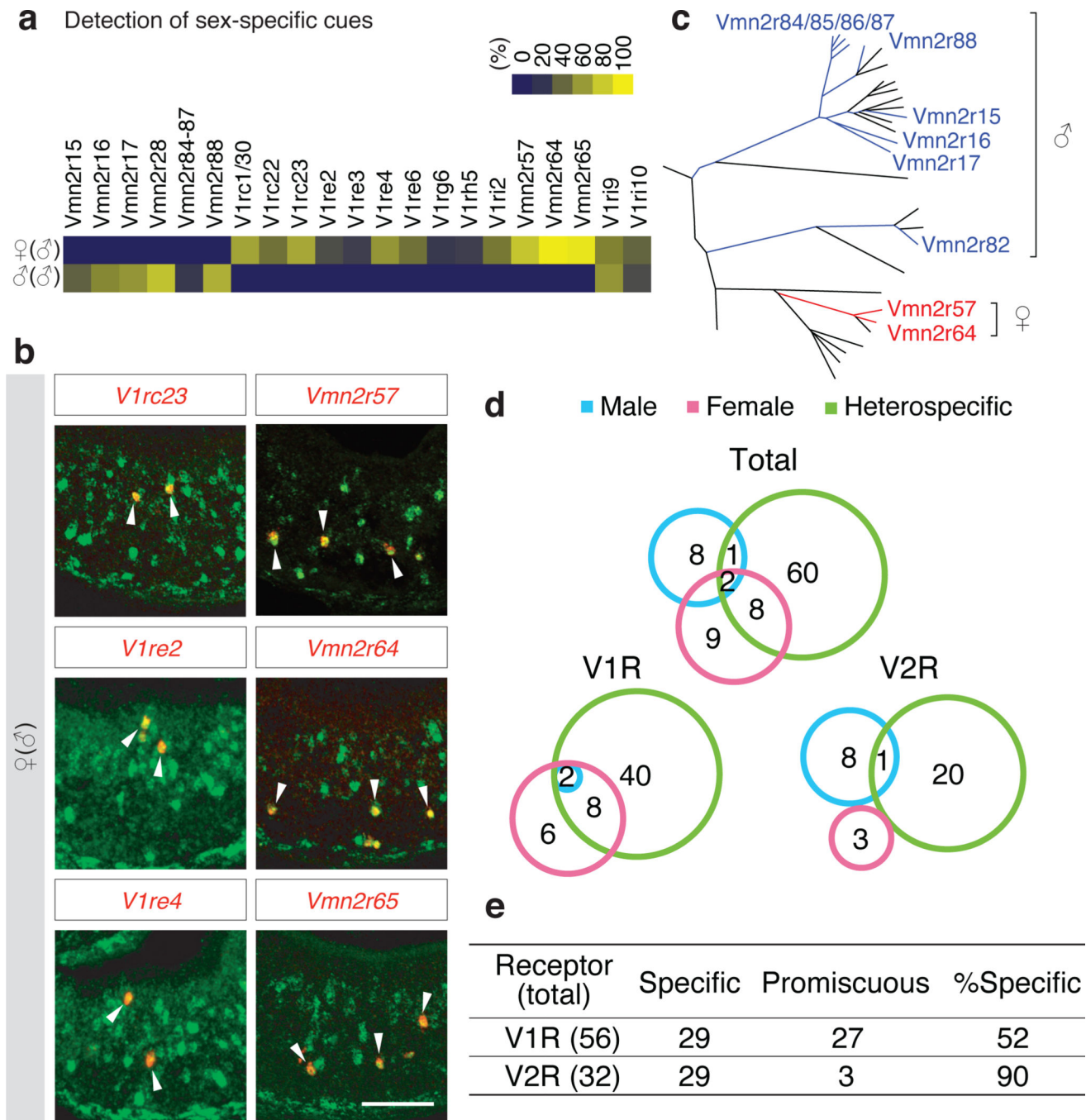


Figure 3. Receptor repertoires to sex-specific cues

a, b, Male and female mouse cues are each detected by a specific subset of V1Rs and V2Rs.

a, Heat maps representing the co-localization between *Egr1* and representative vomeronasal receptor genes (yellow 100%, blue 0% overlap). **b,** In situ hybridization of *Egr1* (green) and individual receptors (red), with arrows marking co-localization of *Egr1* and receptor signals. The scale bars represent 100 μ m. **c,** Clade organization of V2Rs detecting male or female cues.

d, Receptors detecting male, female, and heterospecific cues are largely distinct. **e,** V1Rs and V2Rs display distinct specificity. The table shows the number of receptors that

detect unique types of cues (specific) versus multiple types (promiscuous) among the following categories: male, female, mammalian non-predator, mammalian predator, reptile, and avian predator.

Author Manuscript

Author Manuscript

Author Manuscript

Author Manuscript

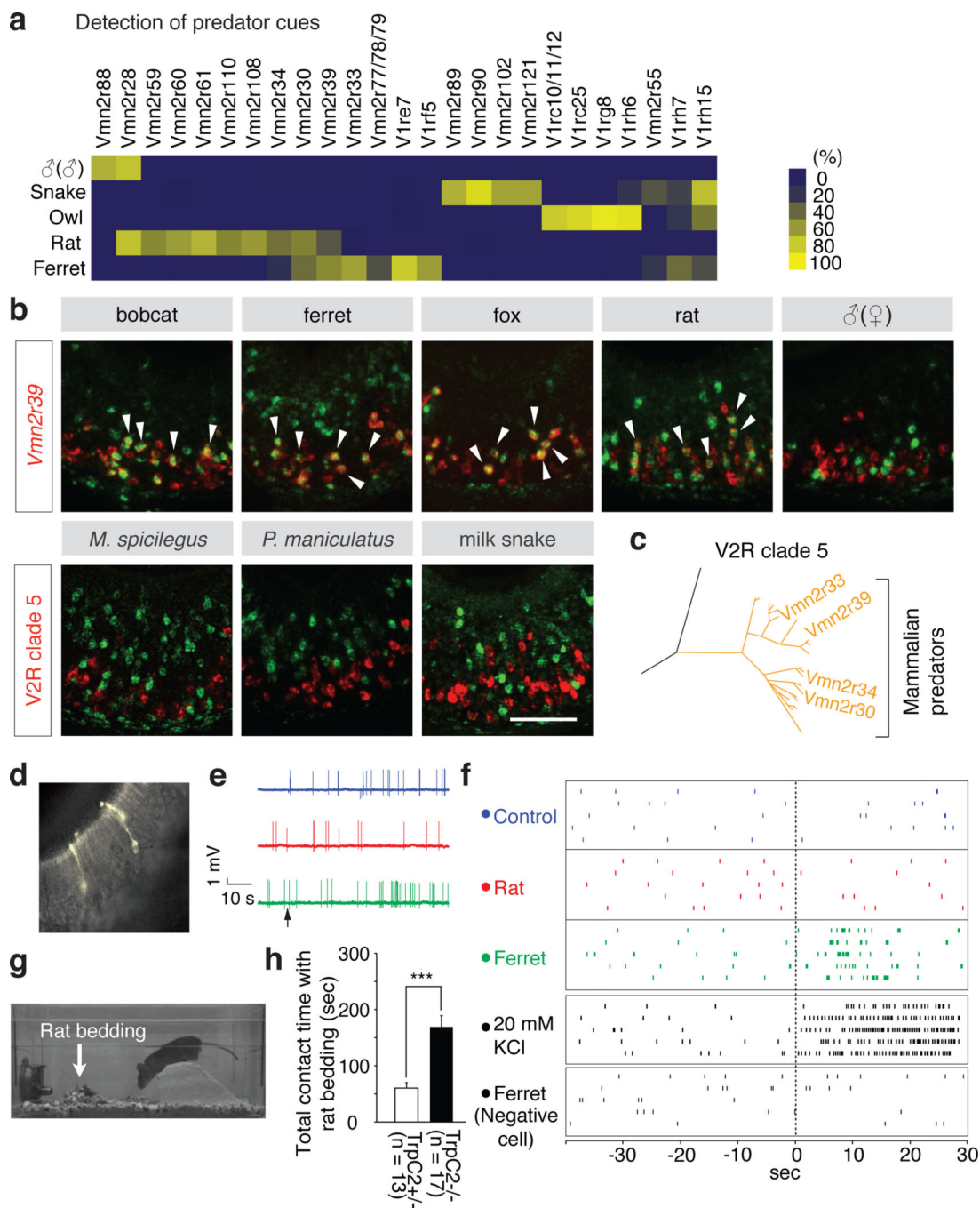


Figure 4. Receptor repertoires to heterospecific cues

a, b, Predator cues are detected by a specific subset of V1Rs and V2Rs. **a,** Heat map representing the co-localization between *Egr1* and representative vomeronasal receptor genes (yellow 100%, blue 0% overlap). **b,** In situ hybridization of *Egr1* (green) and vomeronasal receptors (red), with arrows marking co-localization of *Egr1* and receptor signals. Bar, 100 μ m. **b,c,** Mammalian predator cues commonly activate V2R clade 5 receptors. Due to high homology among V2R clade 5 genes, the Vmn2r30, 33, 34, 39 probes detect multiple receptors. **d,** Fluorescence image showing a patched V1rh7-YFP neuron. **e,**

Loose-patch recordings of a V1rh7-YFP neuron. The arrow indicates perfusion start. **f**, Spike raster for three different VNO neurons showing responses of a V1rh7-YFP neuron and a V1Rh7-YFP negative neuron. The stimulus perfusion started at -30 sec and lasted 20 seconds. **g, h**, Rat bedding (arrow) elicits robust avoidance behaviors in control TrpC2^{+/-} mice, but significantly less in TrpC2^{-/-} mice lacking VNO activity. *** indicates p<0.0001 (two tailed Student's t-Test). Error bars show s.e.m. (TrpC2^{+/-}, n=13, TrpC2^{-/-}, n=17).

Author Manuscript

Author Manuscript

Author Manuscript

Author Manuscript

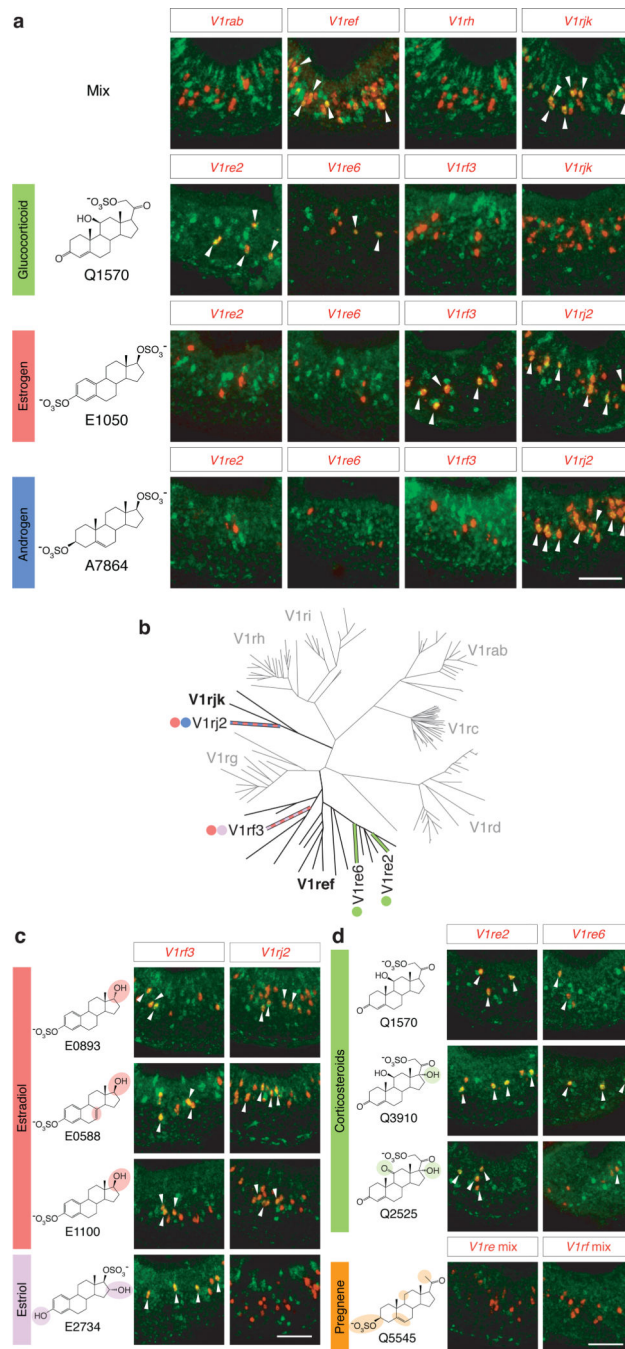


Figure 5. Sulfated steroids detection by V1Rs

a, V1Ref, and V1Rjk clade specific probes (red) co-localize with *Egr1* (green) after VNO stimulation by a mix of steroids containing the glucocorticoid Q1570, the estrogen E1050, and the androgen A7864. Each of these compounds elicits activity in distinct populations of vomeronasal neurons (*V1re2*, *V1re6*, *V1rf3*, and *V1rj2*), also represented in the molecular tree of V1R receptors (**b**). **c**, The three distinct estradiols activate both *V1rf3* and *V1rj2*

while the estriol only activates V1rf3. **d**, The sulfate group position in pregnenes determine the specificity of ligand detection by V1re2 and V1re6. Bar, 100 μ m.

Author Manuscript

Author Manuscript

Author Manuscript

Author Manuscript